Journal of Power Sources 195 (2010) 7230–7233

Contents lists available at ScienceDirect

Journal of Power Sources

journal homepage: www.elsevier.com/locate/jpowsour

Short communication

High performance solid oxide fuel cells based on tri-layer yttria-stabilized zirconia by low temperature sintering process

Ze Liu[a], Zi-wei Zheng[a], Min-fang Han[a,*], Mei-lin Liu[b]

[a] Union Research Center of Fuel Cell, School of Chemical & Environment Engineering, China University of Mining & Technology (CUMTB), Beijing 100083, China
[b] School of Materials Science and Engineering, Georgia Institute of Technology, 771 Ferst Drive NW, Atlanta, GA 30332, United States

ARTICLE INFO

Article history:
Received 20 April 2010
Received in revised form 31 May 2010
Accepted 31 May 2010
Available online 8 June 2010

Keywords:
Tri-layer yttria-stabilized zirconia
Tape casting
Two-step sintering
Infiltration

ABSTRACT

Performance of solid oxide fuel cells (SOFCs) depends critically on the composition and microstructure of the electrodes. It is fabricated a dense yttria-stabilized zirconia (YSZ) electrolyte layer sandwiched between two porous YSZ layers at low temperature. The advantages of this structure include excellent structural stability and unique flexibility for evaluation of new electrode materials for SOFC applications, which would be difficult or impossible to be evaluated using conventional cell fabrication techniques because of incompatibility with YSZ under processing conditions. The porosity of porous YSZ increases from 65.8% to 68.6% as the firing temperature decreased from 1350 to 1200 °C. The open cell voltages of the cells based on the tri-layers of YSZ, co-fired using a two-step sintering at 1200 °C, are above 1.0 V at 700–800 °C, and the peak power densities of cells infiltrated LSCF and Pd-SDC electrodes are about 525, 733, and 935 mW cm^{-2} at 700, 750, and 800 °C, respectively.

© 2010 Elsevier B.V. All rights reserved.

1. Introduction

Solid oxide fuel cells (SOFCs) are the most efficient devices yet invented for conversion of chemical fuels directly into electrical power [1]. Yttria-stabilized Zirconia (YSZ) is currently the most popular solid electrolyte used in SOFCs, which is normally densified at high temperatures in the range of 1300–1700 °C (typically 1400 °C). High sintering temperatures decrease the porosity of electrode in many cell configurations, and also result in coarse-grained microstructures having poor mechanical properties [2]. Therefore, it is benefit to obtain low-cost electrolyte from lowering the sintering temperature.

There are various processing methods and techniques that can be used to reduce the sintering temperature of electrolyte, e.g. some deposition methods [3–6], metal oxide doped in electrolyte [7–9], modified sintering processes [10,11], co-shrinkage of electrolyte/porous electrode [12]. Hobein et al. deposited 1–2 μm YSZ film at 500 °C by pulsed laser deposition, then densified the film at 1200 °C for 3 h [3]. And they also deposited 1–10 μm dense YSZ film on NiO-YSZ substrated by DC sputtering at 500–700 °C [4]. Dahl et al. prepared YSZ film by three different sintering techniques. The relative densities of YSZ films fabricated by hot pressing (HP) at 1250 and 1200 °C were about 97% and 93.6%, respectively, and fabricated by spark plasma sintering (SPS) at 1250 °C is about 99.5% [5]. Perednis and Gauckler prepared 200 nm YSZ film by spray pyrolysis at 500 °C for 2 h [6]. All these deposition methods can obtain dense thin electrolyte film, but not be used as mass-production technology of SOFCs for the high fabrication cost. Some other researchers select sintering aids to reduce the sintering temperature. Bi_2O_3-doped YSZ can be densified by conventional sintering at 1300 °C for 2 h, and by microwave sintering at 1100 °C for 30 min [7]. The relative density of Co doped YSZ sintered at 1200 °C is close to full density [8]. The relative density of transitional metal, Ni doped YSZ was sintered at 1250 °C for 5 h is higher than 95%, and Mn and Fe doped YSZs were sintered at 1250 °C for 5 h, are between 90% and 95% [9]. Whereas some of the doped elements tend to form unwanted compounds with the electrodes [8]. Recently, Han et al. developed a new three-step sintering of YSZ at 1250–1300 °C with a relative density of about 97% [10,11]. Liu and co-workers [12] indicated that porous anode layer ($NiO–Ba(Zr_{0.1}Ce_{0.7}Y_{0.2})O_{3-\delta}$) has effect on densification of thin electrolyte $Ba(Zr_{0.1}Ce_{0.7}Y_{0.2})O_{3-\delta}$ during high temperature co-sintering, which reduces sintering temperature to a relative low range. Combined modified sintering processes and co-shrinkage of electrolyte/porous electrode, we expect to obtain dense YSZ below 1250 °C by conventional sintering process.

Tape casting is a cost-effective process for fabrication of thick ceramic films [13] and can also be easily adapted for fabrication of multiple layers, for example, porous and dense layers of the same or similar materials can be laminated by isostatic pressing, followed by co-firing process [14]. Meanwhile, its scalability and

* Corresponding author at: Box 8, Xueyuan Rd Ding 11, Haidian District, Beijing, PR China. Tel.: +86 10 62341427.
E-mail address: hanminfang@sina.com (M.F. Han).

0378-7753/$ – see front matter © 2010 Elsevier B.V. All rights reserved.
doi:10.1016/j.jpowsour.2010.05.062

Table 1
The porosity and shrinkage of tri-YSZ sintered at different temperatures.

Samples	1200 °C × 10 h	1250 °C × 10 h	1300 °C × 10 h	1350 °C × 5 h
Porosity of porous layer (%)	68.6	67.2	65.8	65.8
Porosity of porous layer in tri-layer YSZ (%)	67.8	66.1	64.4	64.4
Shrinkage of tri-layer YSZ (%)	18.8	20.4	20.8	20.8

long standing success make it an attractive approach for low-cost manufacturing of solid oxide fuel cell (SOFC) components such as electrolyte, electrode, and interconnect [15]. For SOFC applications, it is desirable to fabricate a dense yttria-stabilized zirconia (YSZ) electrolyte layer sandwiched between two porous YSZ layers (tri-layer YSZ matrix) [16–21], then induce active electrode materials in porous YSZ layers to obtain full cell. Low anode overpotentials could be achieved by thin functional layer on the order of 10 μm [22], so the thin porous layer (~50 μm) of tri-layer YSZ matrix is used as anode, and thick porous layer (~300 μm) is used as cathode.

In recent years, strontium- and cobalt-doped lanthanum ferrites, $La_xSr_{1-x}Co_yFe_{1-y}O_{3-\delta}$ (LSCF), have attracted much attention as cathode for intermediate and low temperature SOFCs [23] because of the high electronic and oxygen ion conductivities at low temperatures. Unfortunately, LSCF reacts with YSZ electrolyte to form resistive phases at temperatures higher than 950 °C [24,25]. A doped CeO_2 layer must be used as a buffer between the LSCF and the YSZ electrolyte [26,27] to avoid reactions between LSCF and YSZ under processing conditions. On the other hand, LSCF can be loaded in the porous YSZ matrix as composite cathode by infiltration. Porous YSZ loaded with 50 wt.% ceria as the anode by infiltration achieved high performance at 800 °C [28]. Anode infiltrated with smaller content of Pd (e.g. 1 wt.% Pd) can provide good performance than some other metals [22]. Therefore doped ceria and Pd can be loaded in porous YSZ matrix as active catalytic anode materials.

In this paper, we report our findings in the fabrication of tri-layer YSZ with one dense layer sandwiched by two porous layers, then sintered at 1200–1350 °C. The relative density of middle YSZ layer is still higher than 95% with lower sintering temperature. And lower sintering temperature results smaller shrinkage and higher porosity of porous YSZ, decreasing the amount of pore formers makes the microstructure robust. Further, the performance of button cell fabricated at low temperature is offered.

2. Experimental

Slurries for tape casting were prepared by dispersing YSZ powder (8 mol% yttria, with a median particle size of 0.114 μm) in mixed ethanol–butanone solvent, caster oil as dispersant, dibutyl phthalate (DBP) as plasticizer, and polyvinyl butyral (PVB) as binder [29]. For porous YSZ layers, graphite powders (Furunda Zirconium Materials Co. Ltd., China) were added as pore formers. Different weight ratios of YSZ to graphite were studied, 50 wt.% graphite was selected to add in porous YSZ slurry.

All slurries were prepared using a two-stage milling process. The slurry consisted of YSZ powders, solvent, and dispersant was initially ball-milled for 8 h prior to addition of other constituents. Ball-milling was then resumed for another 40 h before tape casting using a tabletop caster (DR-150, Japan). A typical tri-layer YSZ structure was formed as follows. First, two porous YSZ layers (50 and 300 μm thick) and a dense YSZ layer (40 μm thick) were cast

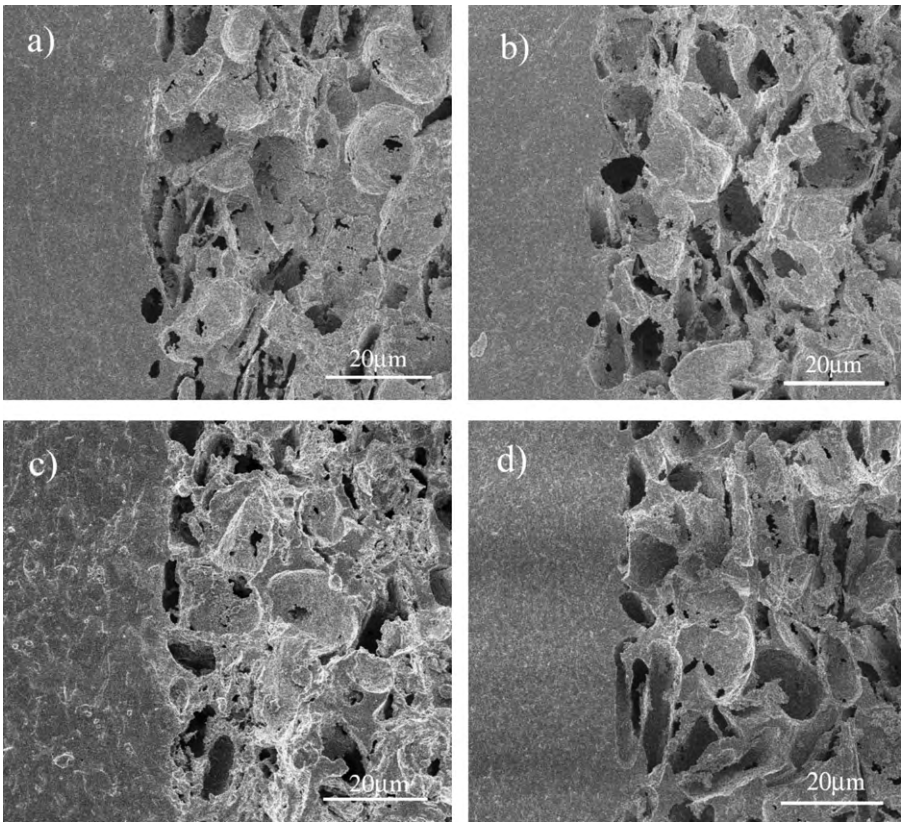

Fig. 1. Microstructure of tri-YSZ sintered by two-step at different temperatures: (a) 1200 °C × 10 h, (b) 1250 °C × 10 h, (c) 1300 °C × 10 h and (d) 1350 °C × 5 h.

separately on a plastic carry film. Then, these tapes were dried in air at room temperature for 12 h. Finally, the tape for dense YSZ was sandwiched between the porous tapes, followed by isostatic pressing at 16 MPa for 20 min using a thermal isostatic press (30T, Shanxi, China). The tri-layer tape was punched to discs, then fired in air at different temperatures: 1200, 1250, 1300 °C for 10 h and 1350 °C for 5 h. The porosities of the fired tapes were measured using the Archimedes method [30]. The microstructural characteristics of the samples (e.g., grain size, pore size, and their distributions) were determined using a scanning electron microscope (FEI XL30 S-FEG).

In this study, LSCF was infiltrated into the porous thick side of the tri-layer YSZ by a solution infiltration process, similar to that used for infiltration of La(Sr, Mn)O_3 (LSM), La(Sr, Co)O_3 (LSC), and La(Sr, Fe)O_3 (LSF) into porous YSZ [21,31,32]. LSCF solutions were prepared by dissolving stoichiometric amounts of $La(NO_3)_3{\cdot}6H_2O$, $Sr(NO_3)_2$, $Co(NO_3)_2{\cdot}6H_2O$, and $Fe(NO_3)_3{\cdot}9H_2O$ in water at a molar ratio of La:Sr:Co:Fe = 0.6:0.4:0.2:0.8. After adding citric acid (the molar ratio of citric acid to metal ions was 1), the clear mixture was stirred for 24 h at 80 °C, with water added to make up for that lost by evaporation. To ensure sufficient fluidity required for infiltration into thick porous YSZ, the concentrations of the solutions were kept at 1.0 mol of metal ions per liter. In order to introduce sufficient amount of LSCF into the porous YSZ, multiple infiltrations were used, followed by firing at 450 °C for 1 h after each infiltration. Finally, 45 wt.% LSCF infiltrated YSZ was fired at 850 °C for 2 h. The thin porous side of tri-YSZ was loaded with 40 wt.% of $Ce_{0.8}Sm_{0.2}O_{2-\delta}$ (SDC) precursor, followed by sintering in air to either 450 °C or 850 °C. Also, 1 wt.% load of Pd was also added to the SDC by infiltration of 0.1 mol L^{-1} aqueous $Pd(NO_3)_2$. For XRD characterization, identical nitrate solutions were also fired to powders under the same condition.

To evaluate the electrochemical performance, the button cells were mounted on an alumina tube as described elsewhere [33]. The area of electrolyte and cathode were about 1.5 cm^2, the external area of anode was 0.2 cm^2, and Ag paste was used as the current collector on the anode. All the performance calculations assumed an active area of 0.2 cm^2. Impedance spectra were typically collected at a small AC perturbation of 10 mV in the frequency range of 0.01–10^6 Hz using IM6 (Zahner). For fuel cell testing, 50 sccm flow rate of humidified hydrogen (3 vol% H_2O, passing through a water bubbler at room temperature) was used as the fuel and ambient air as the oxidant.

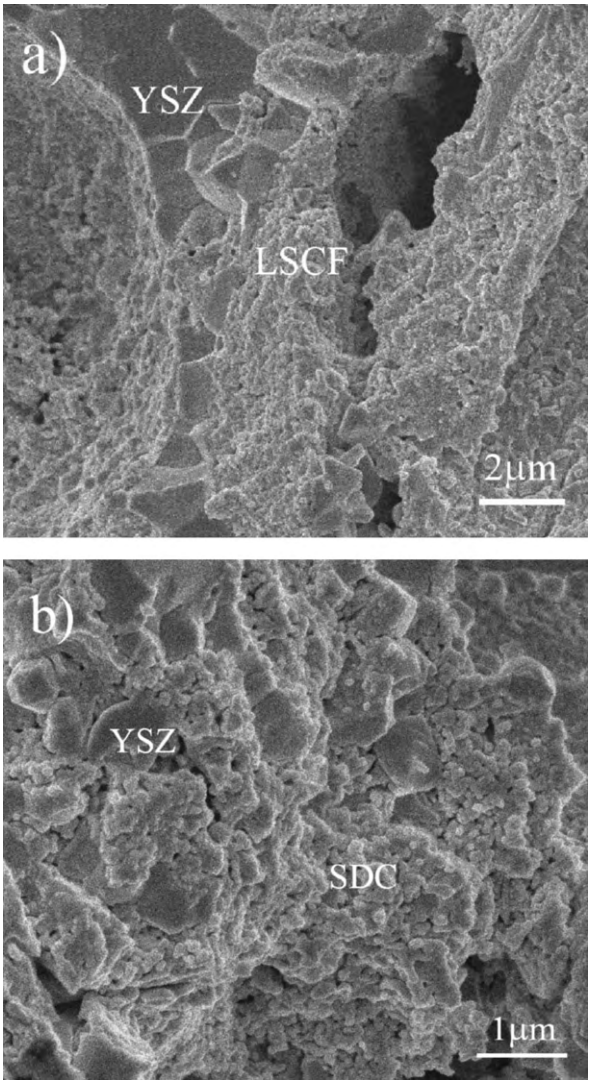

Fig. 2. LSCF and Pd-SDC infiltrated in 1200 °C sintered porous YSZ and calcined at 850 °C: (a) LSCF in porous YSZ and (b) Pd-SDC in porous YSZ.

3. Results and discussion

Based on the previous research [10,11], YSZ tapes were sintered at 1250 °C for 10 h by two-step sintering. The green tape was firstly sintered at 1000 °C for 2–10 h, then raised to 1250 °C at the rate of 1 °C min^{-1}, finally it was fired for 10 h. The relative density of YSZ pellets with 200 μm thickness is about 97%. Similar sintering process was applied on tri-layer YSZ structures. The green tapes of YSZ were first sintered at 1000 °C for 2–10 h, and then the temperature was raised at a rate of 1 °C min^{-1} to 1200–1350 °C. The microstructures of tri-layer YSZ fired at different temperature were shown in Fig. 1. In general, the interfaces of porous YSZ/dense YSZ showed excellent bonding and no pinhole were seen in the dense layer. Table 1 shows the porosity of single porous YSZ and porous YSZ in the tri-layer YSZ structures, respectively, and shrinkage of the tri-layer YSZ structures sintered at different temperatures. The porosities of single porous YSZ and porous YSZ in tri-layer YSZ increased from 65.8% and 64.4% to 68.6% and 67.8%, respectively, when the sintering temperature decreased from 1350 to 1200 °C. As the sintering temperature was lowered, the porosity increased whereas the shrinkage decreased. According to Harmer and Brook [34], at higher sintering temperatures, e.g. 1350–1450 °C, YSZ electrolyte densification is controlled by grain boundary migration and diffusion. At relatively low temperature, e.g. 1200–1300 °C, densification of YSZ electrolyte is controlled mainly by grain boundary diffusion, leading to more small grains. Further more, the densification of the middle YSZ layer is assisted during sintering by the shrinkage of the two outer layers. Tri-layer YSZ structures obtained at 1200 °C for 10 h was a dense layer (~97% relative density) sandwiched between two porous layers with porosity of ~67.8%. Thus, the densification temperature of YSZ was reduced to 1200 °C.

Fig. 2 shows a cell based on a tri-layer YSZ structure sintered at 1200 °C, infiltrated with LSCF and Pd-SDC. The infiltrated LSCF and Pd-SDC particles are about 50–150 nm, and the thickness of LSCF and Pd-SDC films are about 1–2 μm. The nano particles were uniformly and sufficiently coated in the porous YSZ backbone. The porosity of tri-layer YSZ cell after infiltration is about 35.5%. Fig. 3 shows pure pervoskite phase for LSCF and fluorite phase for SDC after fired at 850 °C, as confirmed by XRD analysis.

Fig. 4 shows the cell voltages and power densities as a function of current density at different temperature for a single cell based on a tri-layer YSZ structure with infiltrated anode and cathode. The open cell voltage of tri-YSZ cell was all above 1.0 V at 700–800 °C, implying that the middle YSZ layer is fully dense after sintering at 1200 °C. The peak power densities of the cell are about 525, 733, and

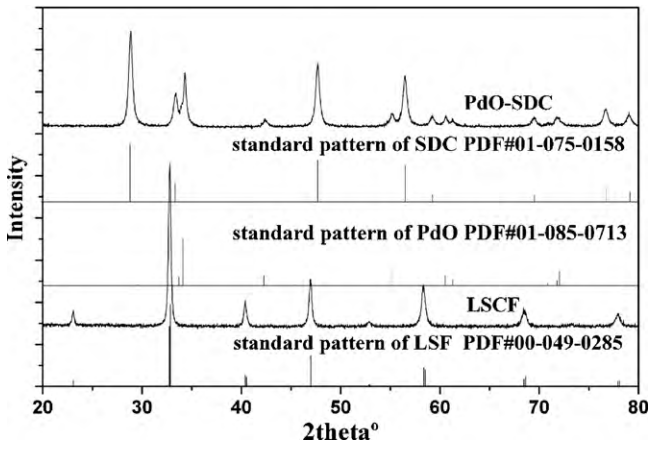

Fig. 3. XRD of LSCF and Pd-SDC infiltrated in porous YSZ.

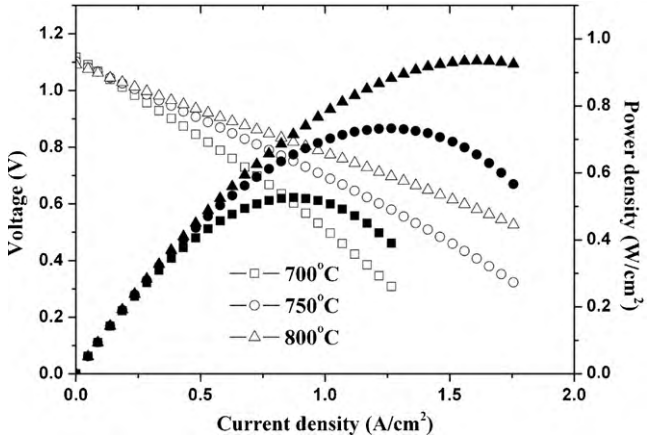

Fig. 4. The performance of cathode supported cell with LSCF and Pd-SDC infiltration.

935 mW cm^{-2} at 700, 750, and 800 °C, respectively. The bulk resistances at 700, 750 and 800 °C were 0.222, 0.190 and 0.144 Ω cm^2, compared to the interfacial resistances in the cell of 0.372, 0.270 and 0.220 Ω cm^2, as shown in Fig. 5. The infiltrated electrodes display high performance most likely due to the unique nanostructures fabricated at relatively low temperatures. According to the value of conductivity of YSZ at 750 °C [11], the contribution to the ohmic resistance from a 40 μm electrolyte was calculated to be ~0.1 Ω cm^2, LSCF in the porous YSZ, as a catalyst and electronic conductor, is catalytically active for oxygen reduction and efficient for current collection [35], which is expected to have negligible ohmic resistance. The calculated ohmic resistance of anode was ~0.09 Ω cm^2, and conductivity of anode was ~0.055 S cm^{-1}, which is higher than the conductivity of Pd-CeO_2 in porous YSZ [22]. SDC is a good non-metallic oxidation catalysts, has better conductivity than CeO_2. Pd-SDC nano particle coating enhanced the surface area

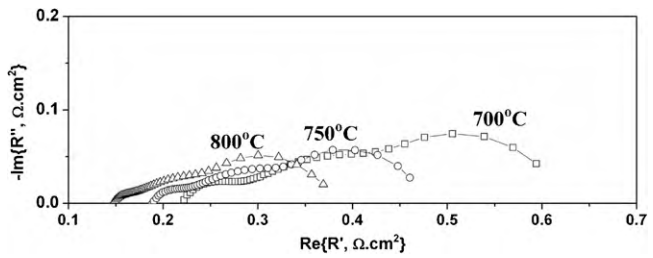

Fig. 5. The impedance spectrum of cathode supported cell with LSCF and Pd-SDC infiltration.

of anode and showed good catalytic properties for fuel oxidation, and SDC is a secondary catalyst in Pd-SDC-YSZ system [36].

4. Conclusion

The tri-layer YSZ structures with one dense (~97% relative density) middle layer sandwiched between two porous (~68% porosity) outer layers was obtained through a two-step co-sintering process at 1200 °C; the densification of the middle layer was assisted by the uniform shrinkage of the two outer porous layers. The peak power densities of the test cells based on these tri-layer YSZ structures infiltrated with LSCF and Pd-SDC are about 525, 733, and 935 mW cm^{-2} at 700, 750, and 800 °C, respectively, suggesting that the tri-layer YSZ structures offer high catalytic activity and cell performance from the infiltrated electrode materials.

Acknowledgement

This material is based upon work supported by NSFC (under grant No. 50730004), MOST (No. 2009DFA6136) and MOE (No. B08010) project.

References

[1] S.C. Singhal, K. Kendall, High Temperature Solid Oxide Fuel Cells: Fundementals, Design and Applications, Elsevier Ltd, Oxford, 2004.
[2] S.P.S. Badwal, Solid State Ionics 76 (1995) 67–80.
[3] B. Hobein, F. Tietz, D. Stover, E.W. Kreutz, J. Power Sources 105 (2002) 239–242.
[4] B. Hobein, F. Tietz, D. Stover, M. Cekada, P. Panjan, J. Eur. Ceram. Soc. 21 (2001) 1843–1846.
[5] P. Dahl, I. Kaus, Z. Zhao, M. Johnsson, M. Nygren, K. Wiik, T. Grande, M.A. Einarsrud, Ceram. Int. 33 (2007) 1603–1610.
[6] D. Perednis, L.J. Gauckler, Solid State Ionics 166 (2004) 229–239.
[7] T.H. Yeh, G.E. Kusuma, M.B. Suresh, C.C. Chou, Mater. Res. Bull. 45 (2010) 318–323.
[8] G.S. Lewis, A. Atkinson, B.C.H. Steele, J. Mater. Sci. Lett. 20 (2001) 1155–1157.
[9] T.S. Zhang, Z.H. Du, S. Li, L.B. Kong, X.C. Song, J. Lu, J. Ma, Solid State Ionics 180 (2009) 1311–1317.
[10] M. Han, X. Tang, J. Wuhan Univ. Technol.: Mater. Sci. 23 (2008) 775–778.
[11] M.F. Han, X.L. Tang, H.Y. Yin, S.P. Peng, J. Power Sources 165 (2007) 757–763.
[12] C. Zuo, S. Zha, M. Hatano, M. Uchiyama, M.L. Liu, Adv. Mater. 18 (2006) 3318–3320.
[13] R.E. Mistler, E.R. Twiname, Tape Casting: Theory and Practice, The American Ceramic Society, Westerville, 2000.
[14] R.J. Gorte, J.M. Vohs, S. McIntosh, Recent developments on anodes for direct fuel utilization in SOFC, Elsevier, Monterey, 2004.
[15] P. Singh, N.Q. Minh, Int. J. Appl. Ceram. Technol. 1 (2004) 5–15.
[16] E. Carlstrom, A. Kristoffersson, Euro Ceramics VII 206-2 (Pt. 1–3) (2002) 205–210.
[17] C. Compson, M.L. Liu, Solid State Ionics 177 (2006) 367–375.
[18] J.B. Davis, A. Kristoffersson, E. Carlstrom, W.J. Clegg, J. Am. Ceram. Soc. 83 (2000) 2369–2374.
[19] S.D. Park, J.M. Vohs, R.J. Gorte, Nature 404 (2000) 265–267.
[20] Y. Huang, J.M. Vohs, R.J. Gorte, Electrochem. Solid State Lett. 9 (2006) A237–A240.
[21] Y.Y. Huang, J.M. Vohs, R.J. Gorte, J. Electrochem. Soc. 152 (2005) A1347–A1353.
[22] M.D. Gross, J.M. Vohs, R.J. Gorte, J. Electrochem. Soc. 154 (2007) B694–B699.
[23] S.P. Jiang, Solid State Ionics 146 (2002) 1–22.
[24] L. Kindermann, D. Das, H. Nickel, Solid State Ionics 89 (1996) 215–220.
[25] H.Y. Tu, Y. Takeda, N. Imanishi, O. Yamamoto, Solid State Ionics 117 (1999) 277–281.
[26] A. Mai, V.A.C. Haanappel, F. Tietz, D. Stover, Solid State Ionics 177 (2006) 2103–2107.
[27] Y. Tao, H. Nishino, S. Ashidate, H. Kokubo, M. Watanabe, H. Uchida, Electrochim. Acta 54 (2009) 3309–3315.
[28] G. Kim, J.M. Vohs, R.J. Gorte, J. Mater. Chem. 18 (2008) 2386–2390.
[29] M.F. Han, L.J. Huo, B.T. Li, S.P. Peng, J. Univ. Sci. Technol. Beijing 12 (2005) 3.
[30] M. Boaro, J.M. Vohs, R.J. Gorte, J. Am. Ceram. Soc. 86 (2003) 395–400.
[31] Y.Y. Huang, K. Ahn, J.M. Vohs, R.J. Gorte, J. Electrochem. Soc. 151 (2004) A1592–A1597.
[32] Y.Y. Huang, J.M. Vohs, R.J. Gorte, J. Electrochem. Soc. 151 (2004) A646–A651.
[33] L. Yang, C.D. Zuo, S.Z. Wang, Z. Cheng, M.L. Liu, Adv. Mater. 20 (2008) 3280.
[34] M.P. Harmer, R.J. Brook, Trans. J. Br. Ceram. Soc. 80 (1980) 147.
[35] M. Shah, J.D. Nicholas, S.A. Barnett, Electrochem. Commun. 11 (2009) 2–5.
[36] B. Wei, Z. Lu, X.Q. Huang, M.L. Liu, K.F. Chen, W.H. Su, J. Power Sources 167 (2007) 58–63.